RESEARCH PAPER

A facile on-demand droplet microfluidic system for lab-on-a-chip applications

Hongbo Zhou · Shuhuai Yao

Abstract We present a facile microfluidic droplet-on-demand (DOD) system in which a pulsed pressure generated by a high-speed solenoid valve is used to control the formation and movement of water-in-oil emulsion droplets in a T-junction microchannel. We investigated the working principle of the DOD system and established a scaling model for the droplet volume in terms of the amplitude and duration of the pulse and the hydraulic resistance of the injection channel. The droplet formation was characterized in three designs at various pressure pulses. The experimental results support our scaling model very well. In the DOD system we developed, nanoliter-volume droplets with a throughput of a few droplets per second were on-demand generated. Moreover, we examined the applicable scope of the DOD system. As examples of practical applications of the DOD system, we demonstrated a digital display module to show droplets formed at a prescribed time and a droplet array with a concentration gradient to show droplets formed with a precise volume. We expect our work can provide design guidelines for a robust DOD system and improve the capabilities of droplet-based microfluidics in 'lab-on-a-chip' systems.

H. Zhou · S. Yao (✉)
Department of Mechanical Engineering, The Hong Kong University of Science and Technology, Hong Kong, China
e-mail: meshyao@ust.hk

H. Zhou
State Key Laboratory of Transducer Technology,
Shanghai Institute of Microsystem and Information Technology,
Chinese Academy of Science, Shanghai, China

1 Introduction

Droplet-based microfluidics offers significant advantages for performing screening and assays (Zheng et al. 2003; Niu et al. 2011), due to their unique features such as reduced sample consumption, less cross-contamination, fast kinetics (Song et al. 2003), and isolation of individual space (Atencia and Beebe 2004; Stone et al. 2004). In order to automate the droplet platform for multi-step, multi-reagent biological and chemical studies, it is essential to generate droplets on demand: at a prescribed time and with a prescribed volume. Formation of picoliter- or nanoliter-volume droplets using water-in-oil emulsion has usually been realized in two configurations: T-junction (Thorsen et al. 2001) and flow-focusing (Anna et al. 2003). Based on these two structures, the most common method for controlling droplet-forming process is achieved by adjusting the inlet pressure or by dictating a constant flow rate using a syringe pump. The correlation between droplet size, distance between droplets, droplet velocity, and formation rate has been extensively studied (Baroud et al. 2010; Garstecki et al. 2006), and it is found that it is almost impossible to obtain any combination of those parameters (Bransky et al. 2008), e.g., in a required volume at a required generation frequency. However, in many biological and chemical assays, precise and flexible control of the formation, composition, and size of individual droplets is often desired. Moreover, the system response time, the time needed for stabilization of droplet formation in these conventional systems, is quite long (e.g., several minutes), which may interfere with the integration and automation of droplet microfluidics in practical applications.

On-demand formation of droplets can greatly facilitate droplet manipulation where the number and size of droplets need to be controlled and droplet synchronization where the droplets need to be adjusted close to each other for fusion or mixing. In order to set up a threshold switch for on-demand operation, a pressure barrier is often needed to regulate the onset of droplet formation. In water-in-oil emulsion, the barrier is usually formed by Laplace pressure at the water/oil interface (Baroud et al. 2010), $P_{\text{barrier}} = 2\gamma(1/W + 1/H)$ with γ the interfacial tension and W, H the width and depth of the microchannel. The water/oil interface can be adjusted by three ways to form DOD system: (1) Controlling the interfacial tension, γ. Local electrodes heating (Tan et al. 2008; Nguyen et al. 2007), optical heating (Baroud et al. 2007) or electrowetting (Malloggi et al. 2008; Gu et al. 2011), have been reported to change the effective interfacial tension and then the pressure barrier. (2) Controlling the dimension of the microchannel, H or W. Pneumatic pressure is applied to a thin and elastic PDMS membrane valve (Lin and Su 2008; Guo et al. 2010; Zeng et al. 2009; Willaime et al. 2006; Galas et al. 2009) to reshape the microchannel and adjust the pressure barrier. (3) Applying a pressure directly to the dispersed phase. Additional pressure by PZT (Bransky et al. 2008; Xu and Attinger 2008; Shemesh et al. 2011) or perturbation by electric field (Fidalgo et al. 2008; Gu et al. 2011) is applied to overcome the barrier. However, for all these methods, additional parts such as electrodes, PDMS membranes, or microactuators are needed to be integrated to achieve the switching function. Recently, a DOD system that utilizes off-chip solenoid valves was reported by Churski et al. (2010) and Dolega et al. (2012), which avoided additional parts on-chip and could interface with any materials-based microfluidic chips. However, their DOD system requires complex integration of a syringe pump, a pressurized container, and two solenoids to control the water and oil flow in microchannels. Delicate modification to the valves and manual integration are needed (Churski et al. 2010), which may cause instability and inconsistency issues in operation. Moreover, their DOD system can only produce a minimum droplet volume of several tens of nanoliter, which is still one order of magnitude higher for typical applications using droplets as isolated compartments or microreactors in microfluidics. Similar idea was also adopted by Jung et al. (2010) to create femtolitre-scale water-in-oil droplets on demand. However, in their system, droplet formation was controlled predominantly by the interfacial tension, rather than the applied pressure or flow rate of the two phases; therefore, the droplet volume could not be freely tuned.

Here, we present a facile DOD system which utilizes only one off-chip solenoid valve and can interface with microfluidic chips of any kinds. We developed a scaling model to describe the related factors (duration and amplitude of the pulse, injection resistances, and so on) contributing to the droplet volume. Microfluidic devices with various channel dimensions were designed and fabricated, and the scaling model was validated by experimental results using these devices. To demonstrate the applications of our DOD system, we show the droplets can be formed and merged at controlled time and volume in a digital display module and a concentration gradient module.

2 Materials and methods

2.1 Working mechanism

As illustrated in Fig. 1, the DOD system is based on a T-junction microchannel for droplet emulsion and a solenoid valve connected to the water phase for generating a pulsed pressure to trigger the onset of droplet injection. A T-junction microchannel is a typical configuration for droplet formation, which consists of a main channel and an injection channel. In principle, to achieve DOD, the dispersed phase should be switched between 'on' and 'off' status arbitrarily. That is, in 'on' status, the dispersed phase is open, while in 'off' status, the dispersed phase is closed. By controlling the 'on' and 'off' status, droplets at a prescribed time and with a prescribed volume can be achieved (Online Resource 2). To facilitate the threshold switch for droplet injection, a nozzle, serving as a capillary stop valve, is introduced at the T-junction to form a pressure barrier (P_{barrier}).

Figure 2a–f shows the snapshots of the droplet formation process upon imposing a pressure pulse on the injection channel. At normal time, P_m and P_i remain constant to
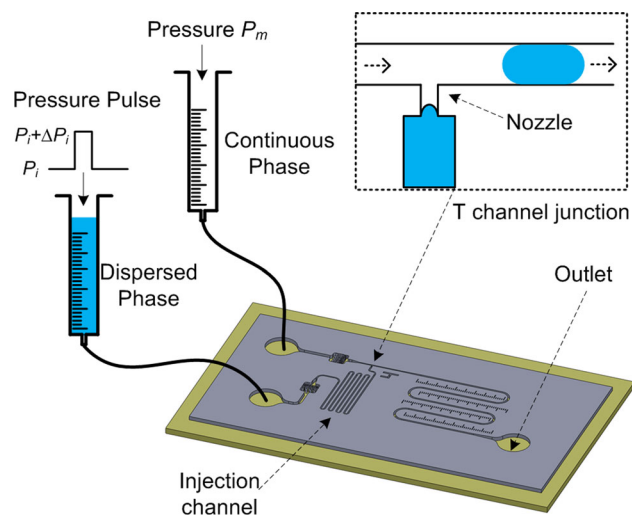

Fig. 1 Schematic illustration of the DOD system. The *inset* is a magnified image of the nozzle at the T-junction
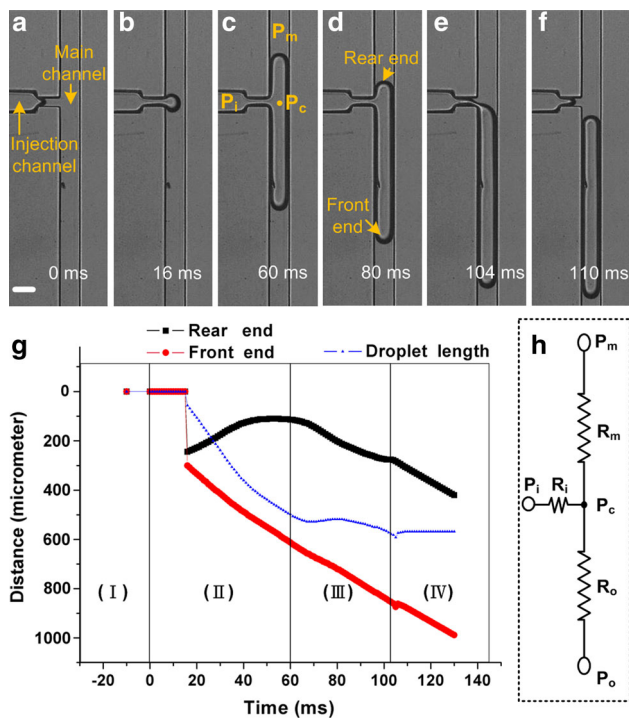
Fig. 2 Principle of the DOD process. A pressure pulse (starts at 0 ms) with duration of 60 ms is applied to the injection channel. **a–f** The snapshot images during one cycle. **g** The location of the rear and front ends, and the length of the droplet during the DOD process. There are four steps during the DOD process: holding (*I*), injecting (*II*), separating (*III*), and recovering (*IV*). **h** Schematic of the flow circuit of the DOD system. The *scale bar* is 60 μm

maintain a water/oil interface at the nozzle (Fig. 2a, g (I)); the DOD system is in 'off' status. The oil phase flows through the main channel with a flow rate of $Q = (P_m - P_o)/(R_m + R_o)$, where R_m and R_o represent the flow resistance of the upstream and downstream, as shown in Fig. 2h. Due to the pressure barrier ($P_{barrier}$) induced by the nozzle, the water phase is confined behind the nozzle (Fig. 2a). Then, the solenoid valve connected to the injection channel is switched between P_i and $P_i + \Delta P_i$, which forms a pressure pulse (ΔP_i) on the water phase and triggers the injecting step (Fig. 2b–d, g (II)). The additional pressure (ΔP_i) overcomes the pressure barrier ($P_{barrier}$), and the water phase is injected from the nozzle and flows into the main channel (Fig. 2b); the system is in 'on' status. During the pulse, the water phase in the main channel extends toward both upstream and downstream, and at the end of the pulse, a water droplet with a volume of V_{pulse} is temporarily formed in the main channel (Fig. 2c). Then, after the pressure pulse ends, the droplet immediately moves down in the main channel (Fig. 2d), and the separating step begins (Fig. 2g (III)). It should be noted that in this step the water phase may keep flowing into or out from the droplet, and the droplet volume is still changing. This process continues until the rear end of the droplet

approaches the edge of the nozzle. Then, the neck becomes longer and thinner (Fig. 2e) until it pinches off. Ultimately, a droplet with a volume of V_{total} is formed in the main channel (Fig. 2f). In the recovering step, the front of water phase rapidly retracts to the nozzle. The system is stabilized under the normal pressures and ready for the repeated DOD cycle. The formed droplet moves downstream in the main channel with a constant volume V_{total}.

A scaling model is proposed (Online Resource 1) to describe the related parameters for the droplet volume, V_{total},

$$V_{total} = \beta_{(Q,\delta P_i, P_\gamma, R_m, R_i)} \cdot \left(\frac{P_{eff}}{R_i}\right) \cdot t_{eff} \tag{1}$$

where P_{eff} and t_{eff} represent the effective amplitude and duration of the pulse, respectively. R_i represents the hydraulic resistance of the injection channel. For a specific device at prescribed conditions (β is constant), we can estimate the relative error (Kotulski and Szczepiński 2010) in V_{total} with respect to the effective amplitude, duration of the pulse, and the injection resistance,

$$\frac{\delta V_{total}}{V_{total}} = \sqrt{\left(\frac{\delta P_{eff}}{P_{eff}}\right)^2 + \left(\frac{\delta t_{eff}}{t_{eff}}\right)^2 + \left(\frac{\delta R_i}{R_i}\right)^2} \tag{2}$$

According to this equation, a pressure pulse with longer duration and larger amplitude can improve the droplet uniformity. However, the volume of the droplet also increases, according to Eq. (1). Therefore, to generate uniform droplets in low volume, a more effective way is to increase the hydraulic resistance of the injection channel.

2.2 Device design, fabrication, and operation

According to Eqs. (1) and (2), the injection channel with high flow resistance is preferred to generate nanoliter (or picoliter)-volume droplets in microfluidics with high uniformity. In our designed devices, the injection channel flow resistance of R_0, $1.5R_0$, and $2.25R_0$ (R_0 represents the reference resistance; in this paper it equals 6×10^{13} kg m^{-4} s^{-1}) was adopted. The nozzle was designed as 30 μm wide and 50 μm deep, which formed a pressure barrier of ~ 4 kPa at the T-junction according to Laplace pressure equation (Baroud et al. 2010). All the channels and patterns in the chips had the same depth of 50 μm.

We fabricated the microfluidic devices in PDMS for its simple fabrication process (although it is not limited to this kind of material). Standard soft lithography procedure was adopted to fabricate the mold for PDMS casting. A negative photoresist (SU-8 2050, MicroChem) was spin-coated and patterned on a silicon wafer. The developed SU-8 pattern yielded a mold for microchannels of 50 μm in depth. The mold was then placed in a desiccator with a

Table 1 Experiment parameters

Injection channel resistance R_i	1.35×10^{14} $(2.25R_0)$ kg m^{-4} s^{-1}
Upstream resistance R_m	9.00×10^{13} kg m^{-4} s^{-1}
Downstream resistance R_o	1.15×10^{15} kg m^{-4} s^{-1}
Main channel pressure P_m	12.41 kPa
Injection channel pressure P_i	13.31 kPa

few drops of trichloro(1H,1H,2H,2H-perfluorooctyl)silane (Sigma-Aldrich) to aid removal of the PDMS layer from the mold. PDMS mixture in a 10:1 ratio of prepolymer and curing agent (Sylgard 184, Dow Corning) was degassed and poured over the mold and cured in an 80 °C oven for an hour. The cast PDMS was then peeled off from the mold, and inlet and outlet holes were punched using a pan head needle on the PDMS replica. The PDMS replica was treated with oxygen plasma and then bonded to another bare PDMS layer to seal the microchannels. The bonded device was heated at 105 °C on a hotplate for 24 h to increase bonding strength and recover the hydrophobicity of the PDMS surfaces.

The oil and water were pumped from syringes (Becton–Dickinson, 3 mL) through the tubing (0.8 mm ID, PTFE, Cole-Parmer) to the two inlets of the microfluidic device. Note that the flow resistances of the syringe and tubing also contribute to the hydraulic resistance R_i of the DOD system, especially when a tubing with small inner diameter is used, and will affect the droplet volume. Constant pressure was applied to each phase using a compressed air system regulated by pressure transducers (2KSNNF01, Marsh Bellofram). A solenoid valve (35A-ACA-DDAA, MAC valves, INC.) was used to impose a pressure pulse on the water phase. The response time of the solenoid valve was 4 ms. In the experiment, the amplitude of the pressure pulse can be adjusted by tuning the pressure transducers, while the duration and start time of the pressure pulse can be adjusted by controlling the solenoid valve. In the experiments, mineral oil (density 840 kg m^{-3}, viscosity 30 mPa s) was used, and no surfactant was added to the oil or water phase. The water/oil interfacial tension was measured as 38 mN m^{-1}.

3 Results and discussion

3.1 Effect of pulse amplitude and duration

We characterized the droplet volume versus the imposed pressure pulse in a microfluidic device. The parameters of the device are listed in Table 1.

To calculate the volume of the generated droplet in the main channel, the droplet was treated as a combination of a cylinder and two semi-torus (Bransky et al. 2008). The data were extracted from CCD images using Matlab codes. In
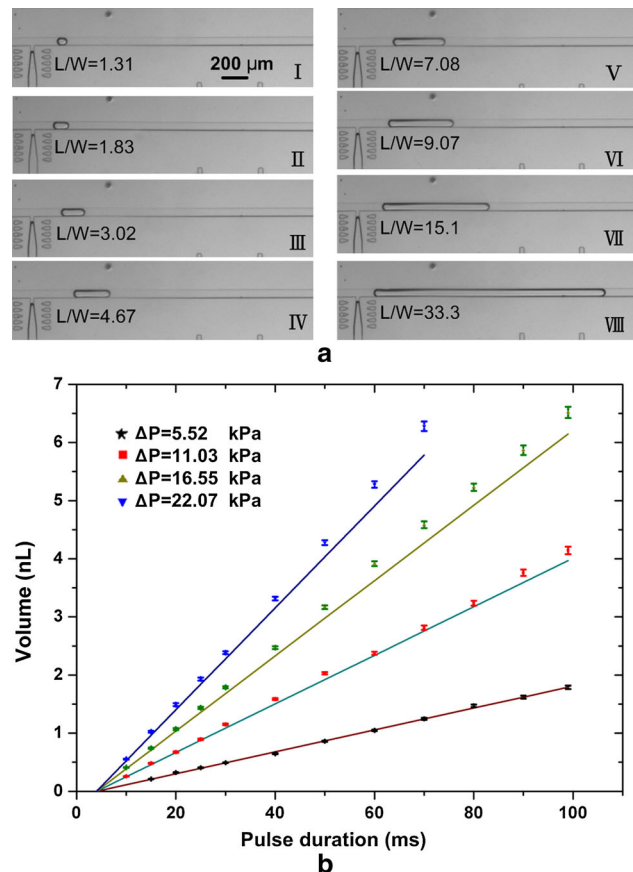

Fig. 3 **a** CCD images showing a wide range of droplet sizes are formed at a constant $\Delta P_i = 11.03$ kPa while varying the pulse duration. **b** The droplet volume varies with pulse duration (10–100 ms) and amplitude (5.52–22.07 kPa). The *solid lines* are the prediction curves for different ΔP_i using Eq. (1)

the experiments, pressure pulses with different amplitude (5.52–22.07 kPa) and duration (10–100 ms) were applied on the injection channel to tune the volume of the generated droplets.

We observed that droplets in a wide range of sizes were generated (Fig. 3a). The length-to-width ratio (L_{drop}/W) varies from 1.31 to 33.3. To predict the droplet volume using Eq. (1), we set the response time of the solenoid valve (4 ms) as the response time (t_{ini}) of the DOD system. As shown in Fig. 3b, the experimental results (dots) match well with the theoretical prediction [by Eq. (1)] and indicate the droplet volume increases linearly with the effective duration of the pulse (t_{eff}). Furthermore, the droplet volume also increases as the amplitude (ΔP_i) of the pressure pulse increases. Therefore, the droplet volume can be tuned by varying both the amplitude and duration of the pressure pulse.

3.2 Effect of injection channel resistance R_i

In many biological or chemical applications, the sample (droplet) volume must be precisely controlled. According
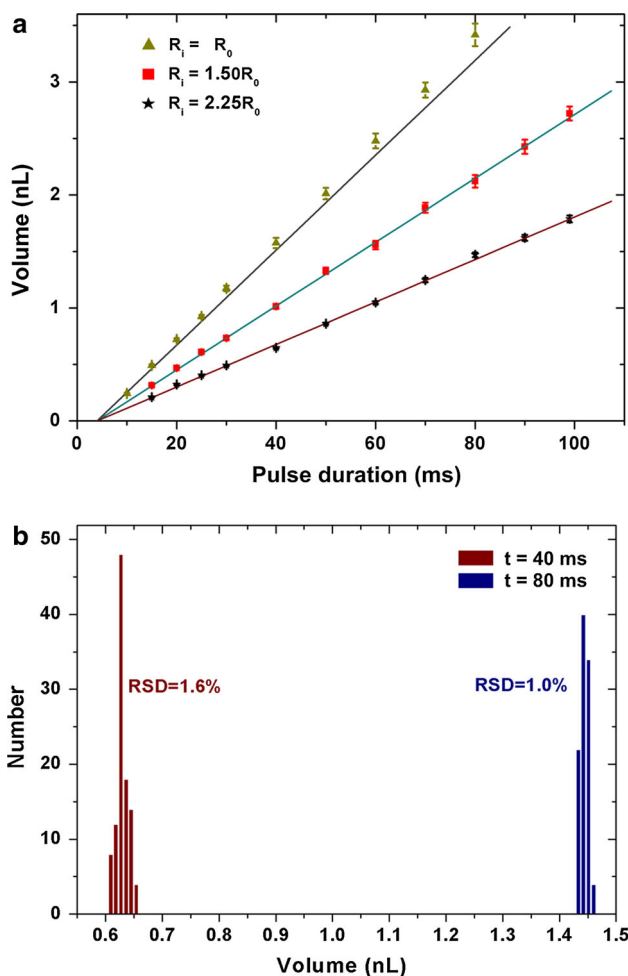
a Droplet volume versus pressure pulse duration for different
flow resistance of the injection channel (R_i). The *solid lines* are
prediction curves for different R_i using Eq. (1). **b** A histogram of
droplets generated by the device with $2.25R_0$ in the injection channel
with pulse duration of 40 and 80 ms

Fig. 4

to our scaling model, the droplet volume depends on the
injection channel resistance R_i. Moreover, from the error
analysis [Eq. (2)], R_i also impacts on the stability of the
DOD system. To verify this effect, we fabricated devices
with various injection channel resistances ($R_i = R_0$, $1.5R_0$,
and $2.25R_0$). All other parameters remained the same as
those in the previous section. In testing these three devices,
pressure pulses with the same amplitude (5.52 kPa) were
applied while the duration stepped from 10 to 100 ms.

In Fig. 4a, it is observed that while the resistance of the
injection channel increases, the droplet volume decreases.
The ratio of the slopes of the curves fits well with the
resistance ratio of the injection channel. We also investi-
gated the standard deviation of the droplet volume for each
data point. Figure 4b shows droplet-volume distribution for
two specific cases (with a pressure pulse of amplitude of
5.52 kPa and duration of 40 and 80 ms, respectively). A
histogram of one hundred droplets is shown for each case.

The mean volumes are 0.64 and 1.44 nL, and the relative
standard deviations (RSD), which indicate the stability of
droplet size, are 1.6 and 1.0 %, respectively. According to
Eq. (2), the RSD value of the DOD droplets can be
improved by increasing the injection channel resistance.
This has been proven by our experiment results. Among the
three devices, the device of highest injection resistance
($2.25R_0$) showed the smallest averaged RSD 1.46 %, while
the values were 2.17 and 2.36 % for devices with $1.5R_0$
and R_0.

We also estimated the resolution of the DOD system.
Here, we define the resolution as the droplet volume with
respect to the duration and amplitude of the pulse. It
is found that the device with the injection channel
resistance of $2.25R_0$ achieves the highest resolution,
3.42 pL ms^{-1} kPa^{-1}. Although the resolution can be fur-
ther improved by increasing the injection channel resis-
tance, larger chip area and higher external pressure are
required as well. Therefore, there is a trade-off between the
resolution and operation cost.

3.3 Droplet characterization

We further studied the relative size of the droplet in terms
of the ratio of the length (L_{drop}) and width of the main
channel (W) versus the capillary number ($C_a = \eta v/\gamma$, where
η and v are the viscosity and velocity of the oil phase, and γ
is the water–oil interfacial tension). As shown in Fig. 5b, a
minimum value of L_{drop}/W is 1.16. This is reasonable
because in the experiment, the capillary number was small
(lower than 0.012) and the value of $\lambda = W_{nozzle}/W$ was
about 0.5, which means that the droplet-forming process
was in 'squeezing' regime (van Steijn et al. 2010; Baroud
et al. 2010; Xu et al. 2008). In this regime, the droplet
should be large enough to obstruct the main channel at the
T-junction to form a sufficient upstream pressure of the
droplet and regularly complete the separation process. This
defines a limitation on the minimum droplet volume of the
DOD system, which is consistent with the minimum value
of 1.16 from Garstecki et al.'s experimental work (2006).

Moreover, according to the capillary number, the sta-
bility diagram can be roughly divided into three regions
(Fig. 5a). When the capillary number is smaller than
0.0012 (region I), due to the low flow rate of the continuous
flow, the system cannot quickly build up a sufficient
upstream pressure to pinch off a droplet. Droplet breakup
process in the orifice becomes irregular, and droplets in
various sizes are produced (Fig. 5b(I)). However, when the
capillary number is larger than 0.0052 (region III), the
pressure upstream increases so fast that the droplets in
the main channel are broken into two or more satellite
droplets (Fig. 5b(III)). When the capillary number falls
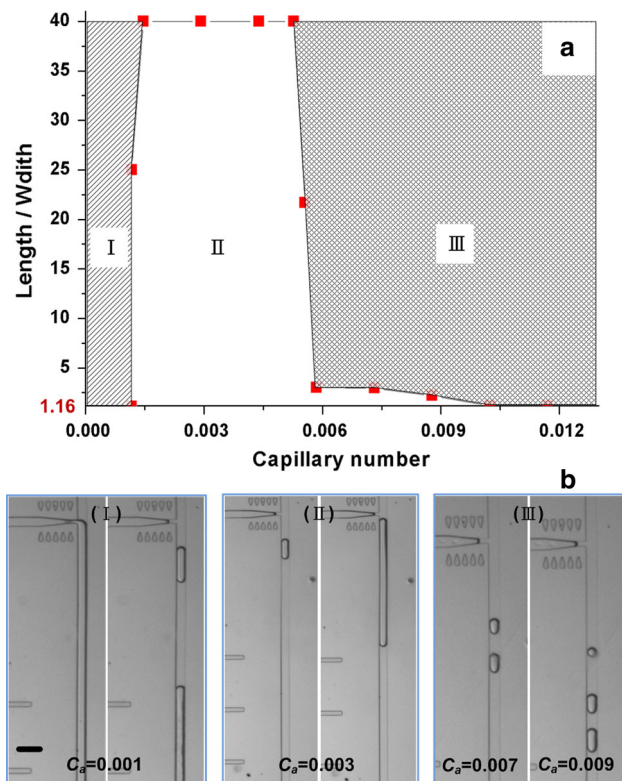within the region II (0.0012–0.0052), droplets can be well

Fig. 5 a Phase diagram correlating the dimensionless length ratio (L_{drop}/W) to the capillary number. Data for dimensionless length ratio larger than 40 are not shown. **b** Images of the generated droplets as the capillary number are increased. The droplets can be categorized in three regions. In region *I*, highly irregular droplets are produced. In region *II*, droplets are well controlled. In region *III*, satellite droplets are formed. The *scale bar* is 150 μm

controlled according to Eq. (1) (Fig. 5b(II)), and the ratio (L_{drop}/W) can be tuned in a wide range from 1.16 to 40. Therefore, to obtain droplets with well-controlled volume, the DOD system need to operate in region II. As the volume of the droplet scales as W^2, in practical designs, we can adjust the width of the main channel at the T-junction to tune the minimum droplet volume. Online Resource 1 gives an example of tuning droplet size by changing the main channel width from 90 to 45 μm.

Another big concern in practical applications of the DOD system is the throughput. Since the solenoid valve is a mechanical valve, its response time is usually several milliseconds (4 ms in our case). Additionally, in the experiments, few hundreds of milliseconds are needed for the inlet loading pressure to be stable after a typical DOD cycle. These factors ultimately limit the throughput of the DOD system to a few droplets per second. Methods (such as adopting a fast recovery pressure source, using a proportional–integral–derivative (PID) controller to optimize the pressure control system, and so on) can reduce the recovery time and therefore enhance the throughput of the DOD system.

3.4 Demonstration

3.4.1 Digital display

To demonstrate the DOD system's ability of generating droplets at a prescribed time, a digital display module in microfluidics was designed. Shown in Fig. 6a is a schematic illustration of the chip designed to achieve the digital display function. In the experiment, a 100-μm-wide serpentine channel was used as the display panel. By sequentially applying pressure pulses at the prescribed time, on-demand droplets were produced accordingly, and the interval (in time and space) between each of the two adjacent droplets in the microchannel can be carefully tuned by coding the start times of the pressure pulses. These droplets moved down along the serpentine channel and resulted in a display of a digital character at a particular moment (Online Resource 3). Figure 6b–k shows digital numbers (0–9) using the same device.

The accuracy of time in control can be estimated. In Fig. 6b–k, it is found that the deviation of the droplet placement from the 'idea' location was within 10 μm. For an average velocity of 2 mm/s in the display channel, an accuracy of 5 ms could be achieved.

3.4.2 Concentration gradient

Forming droplets with accurate and controllable reagent concentration is useful for biological assay or screening. Here, a concentration gradient in a droplet array was demonstrated with the aid of the DOD system. Shown in Fig. 7a is a schematic illustration of a microfluidic device designed to achieve concentration gradients by controlling the fusion of two droplets. In the device, firstly, a pair of droplets (reagent A and B, each with a known concentration) was generated by the DOD system. Then, this pair of droplets was merged in a passive merging chamber that contained two rows of blockage posts (Niu et al. 2008) and formed a new droplet. Finally, the merged droplets were transferred out of the merging chamber and trapped in an array to facilitate observing or other experiments in sequence (Online Resource 4). By generating droplets with different volumes, the volume ratio (A/B) of the two droplets was precisely adjusted before merging (Fig. 7b, d), which ensured the concentration in the new droplet be readily and accurately determined (Fig. 7c, e).

In the experiments, 3 μM FITC and pure water were used to show the concentration gradient effect in the merged droplets. Eight pairs of droplets with volume ratios of 0:8, 1:7, 2:6, 3:5, 4:4, 5:3, 6:2, and 7:1 were generated, respectively, and merged correspondingly. Then, the merged droplets were trapped subsequently in the chamber array (Fig. 7f, g). To obtain the calibration curve, samples
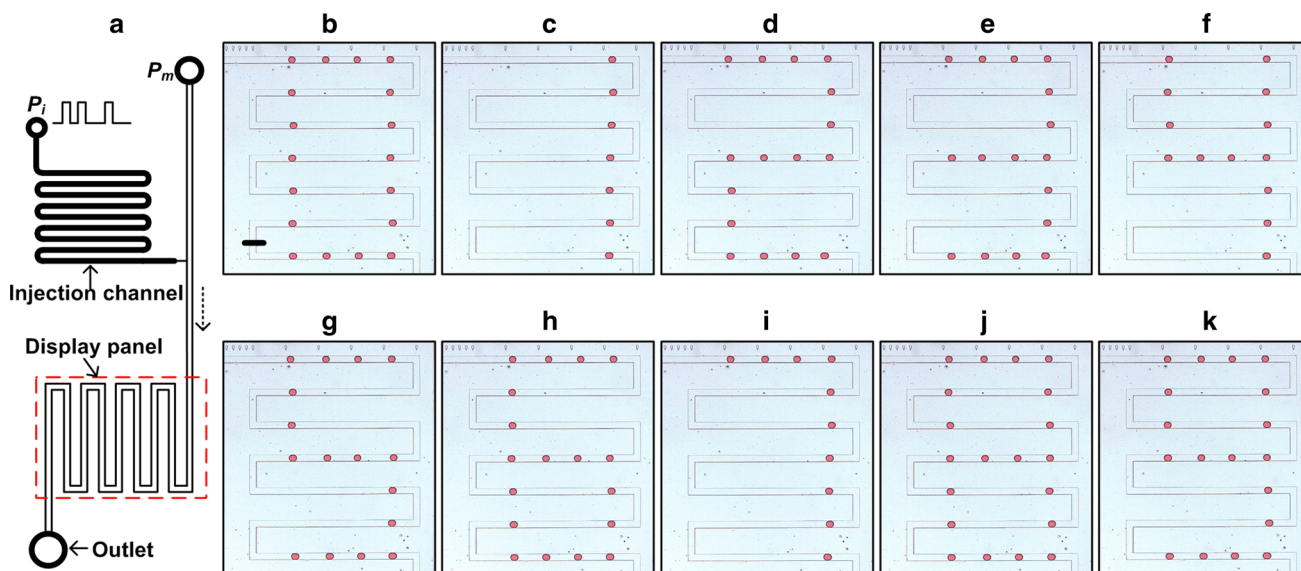
Fig. 6 a Schematic illustration of the chip for digital display. **b–k** Digital display of the numbers, 0–9. The width of the microchannel is 100 μm. The resistance of the injection channel is $2.25R_0$. A pressure pulse ($\Delta P_i = 5.52$ kPa and $t = 40$ ms) is applied to generate droplets with a volume of ~0.65 nL. The average velocity in the display channel is 2 mm/s. The *scale bar* is 300 μm
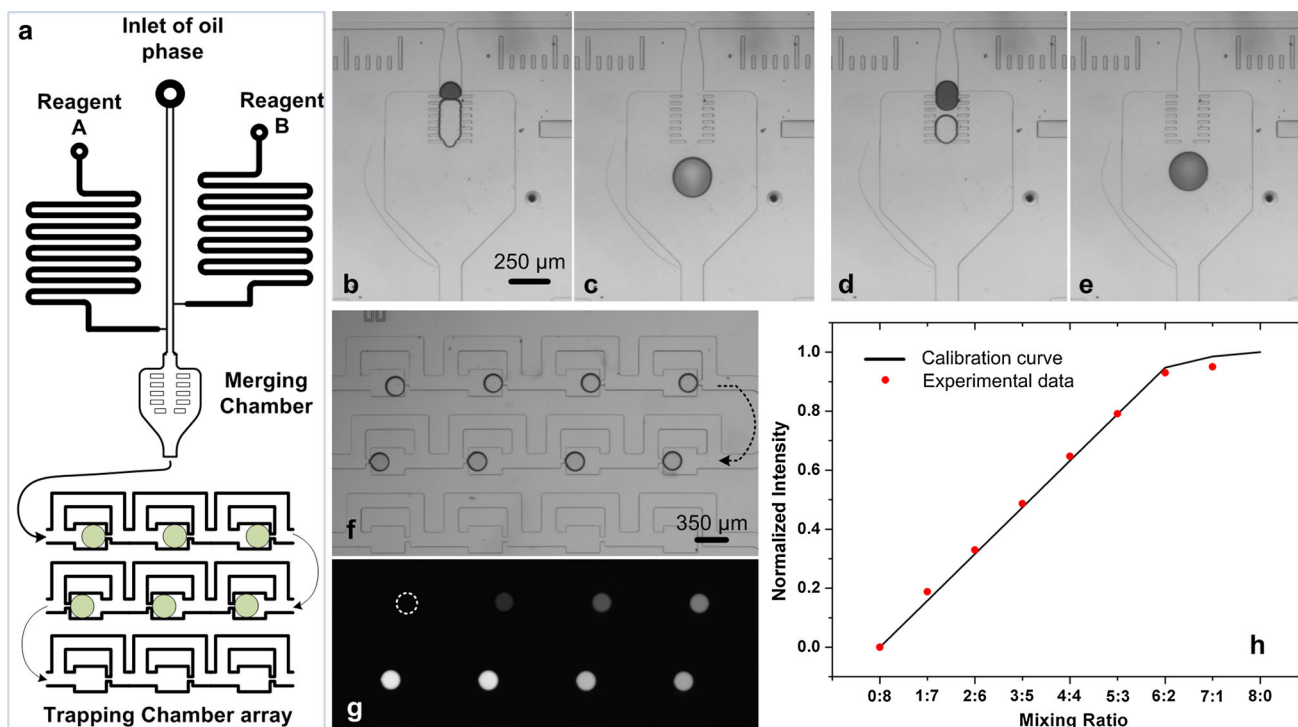

Fig. 7 a Schematic illustration of the chip for generating an array of droplets with a concentration gradient. This chip includes a DOD system for forming droplets *A* and *B*, a merging element, and a trapping chamber array. **b–e** In the merging chamber, a pair of droplets with various volume ratios are merged passively into one droplet. **f** A CCD image showing droplets of ~1.6 nL labeled with FITC in the trapping chamber array. **g** A fluorescence image showing the droplets with a concentration gradient and **h** a calibration curve and the normalized fluorescence intensity of the mixed solutions in the droplet array

with the same mixing ratios were premixed and injected into the same device to form the droplets in the chamber array. Fluorescence images for each sample were taken, and then, the fluorescence intensity at each concentration was extracted and normalized. The results of the concentration gradient array are in excellent agreement with the calibration curve (Fig. 7h), which validate that the DOD system can form a droplet with a precise volume.

Compared with the conventional methods that form different concentrations in droplets or microchannels by adjusting the flow rate of different reagents (Lin et al. 2004; Zheng et al. 2003; Yeh et al. 2011), the distinct features of the DOD system include no dead volume and a short response time. From Fig. 7f, it is clearly observed that the concentration controlling process starts from the first chamber, which indicates zero dead volume. This is very important for the situation when expensive reagents or tiny samples are in use.

3.5 Conclusion

In this paper, we present a simple and adaptive DOD microfluidic system based on the application of a high-speed valve. Compared with the previously developed DOD technology using integrated pneumatic microvalves, our design is simple in fabrication and flexible in operation. By tuning the pulsed pressure imposed by the valve or modifying the hydraulic resistance of the injection channel in the device, the formation of nanoliter droplets with high uniformity can be precisely controlled in time and volume. The droplet volume, length-to-width ratio, and size uniformity were characterized in different designs and operational conditions. The results agree with our scaling law developed using a simple hydraulic model. We demonstrated a digital display and a concentration gradient using the on-demand droplets. We believe our improved DOD system will find important applications of droplet-based microfluidics in automated biological assay, protein crystallization, dose screening, and nanomaterial synthesis.

References

Anna SL, Bontoux N, Stone HA (2003) Formation of dispersions using "flow focusing" in microchannels. Appl Phys Lett 82:364

Atencia J, Beebe DJ (2004) Controlled microfluidic interfaces. Nature 437(7059):648–655

Baroud CN, de Saint Vincent MR, Delville J-P (2007) An optical toolbox for total control of droplet microfluidics. Lab Chip 7(8):1029–1033

Baroud CN, Gallaire F, Dangla R (2010) Dynamics of microfluidic droplets. Lab Chip 10(16):2032–2045

Bransky A, Korin N, Khoury M, Levenberg S (2008) A microfluidic droplet generator based on a piezoelectric actuator. Lab Chip 9(4):516–520

Churski K, Korczyk P, Garstecki P (2010) High-throughput automated droplet microfluidic system for screening of reaction conditions. Lab Chip 10(7):816–818

Dolega ME, Jakiela S, Razew M, Rakszewska A, Cybulski O, Garstecki P (2012) Iterative operations on microdroplets and continuous monitoring of processes within them; determination of solubility diagrams of proteins. Lab Chip 12(20):4022–4025

Fidalgo LM, Whyte G, Bratton D, Kaminski CF, Abell C, Huck WTS (2008) From microdroplets to microfluidics: selective emulsion separation in microfluidic devices. Angew Chem Int Ed 47(11):2042–2045

Galas J-C, Bartolo D, Studer V (2009) Active connectors for microfluidic drops on demand. New J Phys 11(7):075027

Garstecki P, Fuerstman MJ, Stone HA, Whitesides GM (2006) Formation of droplets and bubbles in a microfluidic T-junction—scaling and mechanism of break-up. Lab Chip 6(3):437–446

Gu H, Murade CU, Duits MH, Mugele F (2011) A microfluidic platform for on-demand formation and merging of microdroplets using electric control. Biomicrofluidics 5:011101

Guo F, Liu K, Ji XH, Ding HJ, Zhang M, Zeng Q, Liu W, Guo SS, Zhao XZ (2010) Valve-based microfluidic device for droplet on-demand operation and static assay. Appl Phys Lett 97(23):233701–233703

Jung S-Y, Retterer ST, Collier CP (2010) On-demand generation of monodisperse femtolitre droplets by shape-induced shear. Lab Chip 10(20):2688–2694

Kotulski Z, Szczepiński W (2010) Functions of Independent random variables. In: Error analysis with applications in engineering, vol 169. Solid mechanics and its applications. Springer, Netherlands, pp 91–105. doi:10.1007/978-90-481-3570-7_4

Lin B-C, Su Y-C (2008) On-demand liquid-in-liquid droplet metering and fusion utilizing pneumatically actuated membrane valves. J Micromech Microeng 18(11):115005

Lin F, Saadi W, Rhee SW, Wang S-J, Mittal S, Jeon NL (2004) Generation of dynamic temporal and spatial concentration gradients using microfluidic devices. Lab Chip 4(3):164–167

Malloggi F, Gu H, Banpurkar A, Vanapalli S, Mugele F (2008) Electrowetting—a versatile tool for controlling microdrop generation. Eur Phys J E 26(1–2):91–96

Nguyen N-T, Ting T-H, Yap Y-F, Wong T-N, Chai JC-K, Ong W-L, Zhou J, Tan S-H, Yobas L (2007) Thermally mediated droplet formation in microchannels. Appl Phys Lett 91(8):084102–084103

Niu X, Gulati S, Edel JB (2008) Pillar-induced droplet merging in microfluidic circuits. Lab Chip 8(11):1837–1841

Niu X, Gielen F, Edel JB (2011) A microdroplet dilutor for high-throughput screening. Nat Chem 3(6):437–442

Shemesh J, Nir A, Bransky A, Levenberg S (2011) Coalescence-assisted generation of single nanoliter droplets with predefined composition. Lab Chip 11(19):3225–3230

Song H, Tice JD, Ismagilov RF (2003) A microfluidic system for controlling reaction networks in time. Angew Chem 115(7):792–796

Stone HA, Stroock AD, Ajdari A (2004) Engineering flows in small devices: microfluidics toward a lab-on-a-chip. Annu Rev Fluid Mech 36:381–411

Tan SH, Murshed SMS, Nguyen NT, Wong TN, Yobas L (2008) Thermally controlled droplet formation in flow focusing geometry: formation regimes and effect of nanoparticle suspension. J Phys D Appl Phys 41(16):165501

Thorsen T, Roberts RW, Arnold FH, Quake SR (2001) Dynamic pattern formation in a vesicle-generating microfluidic device. Phys Rev Lett 86(18):4163–4166

van Steijn V, Kleijn CR, Kreutzer MT (2010) Predictive model for the size of bubbles and droplets created in microfluidic T-junctions. Lab Chip 10(19):2513–2518

Willaime H, Barbier V, Kloul L, Maine S, Tabeling P (2006) Arnold tongues in a microfluidic drop emitter. Phys Rev Lett 96(5):054501

Xu J, Attinger D (2008) Drop on demand in a microfluidic chip. J Micromech Microeng 18(6):065020

Xu J, Li S, Tan J, Luo G (2008) Correlations of droplet formation in T-junction microfluidic devices: from squeezing to dripping. Microfluid Nanofluid 5(6):711–717

Yeh C-H, Chen Y-C, Lin Y-C (2011) Generation of droplets with different concentrations using gradient-microfluidic droplet generator. Microfluid Nanofluid 11(3):245–253

Zeng S, Li B, Su X, Qin J, Lin B (2009) Microvalve-actuated precise control of individual droplets in microfluidic devices. Lab Chip 9(10):1340–1343

Zheng B, Roach LS, Ismagilov RF (2003) Screening of protein crystallization conditions on a microfluidic chip using nanoliter-size droplets. J Am Chem Soc 125(37):11170–11171